Hindawi
Geofluids
Volume 2019, Article ID 3183816, 10 pages
https://doi.org/10.1155/2019/3183816

Research Article

Experimental Study on the Effect of Gas Pressure on Ultrasonic Velocity and Anisotropy of Anthracite

Bo Wang[1], **Jialin Hao**[1], **Shengdong Liu**[1], **Fubao Zhou**[2], **Zhendong Zhang**[1], **Heng Zhang**[1] and **Huachao Sun**[1]

[1]*State Key Laboratory for Geomechanics and Deep Underground Engineering and School of Resource and Earth Science, China University of Mining and Technology, Xuzhou, Jiangsu 221116, China*
[2]*School of Safety Engineering, China University of Mining and Technology, Xuzhou, Jiangsu 221116, China*

Correspondence should be addressed to Bo Wang; wbsyes@126.com

Received 12 March 2019; Revised 25 May 2019; Accepted 17 July 2019; Published 19 August 2019

Academic Editor: Lionel Esteban

To research the elasticity of gas-bearing coal fluid-solid two-phase medium with seismic exploration method is critical to the prevention of gas disasters. To investigate the elasticity, the ultrasonic elastic test of anthracite samples under different gas pressures was carried out and the ultrasonic velocity and anisotropy of the samples were analyzed in this study. The results show that the velocities (P- and S-waves) decrease in turn in the strike, dip, and vertical directions. However, a negative linear correlation is proved to exist between ultrasonic velocity and gas pressure. With the increase of gas pressure, the anisotropy degree of both the P-wave and the S-wave of the samples decreases but the declining degree of the P-wave is greater than that of the S-wave. In addition, the decrease in velocity and the anisotropy degree of the P-wave is greater than that of the S-wave, indicating that the P-wave is more sensitive to gas pressure changes in terms of velocity and its anisotropy degree.

1. Introduction

The condition of complex multiphase medium, which is composed of the material composition and structure of coal and fluid gas, is the bottleneck for the mechanism study of coal and the prevention of gas disasters [1]. So far, the information of material composition and structure of coal is obtained mainly through in situ coal seam drilling. However, drilling is costly, laborious, and time-consuming, and thus, it is urgent to analyze the composition and structure characteristics of coal from small-scale laboratory physical experiments. The coal ultrasonic testing technology, thanks to its good orientation, strong directivity, and outstanding penetration ability [2], is used to measure the elastic parameters of coal samples [3]. Although there is a great difference between the ultrasonic wave and the actual seismic frequency band, ultrasonic measurement is significant for actual low-frequency seismic exploration [4].

In China, when the gas pressure in a coal seam reaches or exceeds 0.74 MPa, the coal seam can be defined as an outburst coal seam and corresponding outburst prevention measures should be taken [5]. For this reason, many scholars have carried out in situ seismic wave tests in coal mines in order to provide guidance for the prevention and control of gas disasters. Their research results showed that the presence of gas would reduce the strength of coal and cause coal seam fracture, which is prone to trigger coal and gas outburst accidents [6–8], and that there is a negative linear correlation between coal seam gas content and single-component seismic wave parameters. Specifically, as the gas pressure increases, the velocities (P- and S-waves) decrease gradually, the inherent dominant frequency of the coal seam decreases, the attenuation coefficient increases, and the quality factor decreases [9–11]. As instructive as the above occurrence rules are, it is still difficult to reveal the mechanism scientifically in that the current researches only focus on single-component seismic data on the single direction. Besides, the complex underground site conditions and various influence factors also increase the complexity of the issue under discussion. Therefore, many scholars have conducted long-term

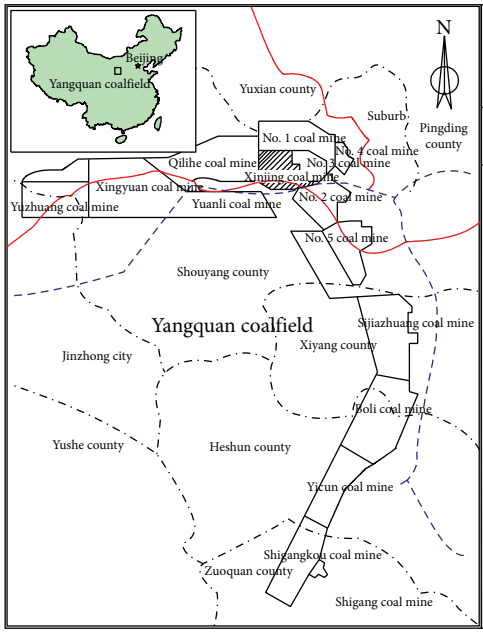

Geology age	Formation	Depth (m)	Thickness (m)	Description	Lithology 1:500
Lower Permian	Shanxi	617.79	7.71	#K7 sandstone	
Upper Carboniferous	Taiyuan	624.12	6.33	Mudstone	
		625.85	1.73	#8 coal	
		630.85	5.00	Silty mudstone	
		639.00	8.15	#K6 medium sandstone	
		641.50	2.50	Silty mudstone	
		642.96	1.46	#9 coal	
		647.66	4.70	Sandy mudstone and mudstone	
		653.46	5.80	Fine sandstone	

Figure 1: Study area location and detailed stratigraphic column of coal-bearing strata in the Yangquan coalfield.

researches on the physical and mechanical properties of coal samples [12–16] and gained some important insights on elasticity. For example, the greater the density of the coal samples is, the larger the velocities (P- and S-waves) become [17]. Under normal temperature and atmospheric pressure conditions, the ultrasonic velocity decreases in turn in the strike direction x, the dip direction y, and the vertical direction z. That is to say, the velocities (P- and S-waves) display azimuthal anisotropy [17, 18]. Moreover, the attenuation of the P-wave is remarkably greater than that of the S-wave with the change of fracture orientation [19, 20].

In summary, many researches have been conducted on the variation law of seismic wave parameters of outburst coal through in situ seismic wave test of coal seam but it is difficult to reveal the mechanism scientifically due to the limitation of site conditions and complex influence factors. Some scholars have studied the ultrasonic elastic parameters and anisotropic characteristics of coal samples such as velocity anisotropy, Poisson's ratio, and attenuation with different degrees of metamorphism under normal temperature and atmospheric pressure conditions through laboratory coal physical experiments. However, the ultrasonic experiments of coal samples are mainly aimed at single-phase solid coal. Considering that gas-bearing coal is a fluid-solid two-phase medium and the limitations of test equipment and conditions, the current related research only focuses on single-phase solid coal and the results are lacking of representativeness and persuasion.

The purpose of this paper is to study the influence of fluid gas on the ultrasonic velocity and anisotropy of coal samples. Therefore, the ultrasonic velocity response characteristics of coal samples under different gas pressures are tested and the effect of gas pressure on the ultrasonic anisotropy of coal samples is analyzed. The research results of this paper may provide some guidance for coal and gas disaster prediction.

2. Sampling and Experiment

2.1. Sample Preparation. The samples in this study were collected at the tunneling face of the Xinjing Coal Mine in the Yangquan coalfield (Figure 1). The Yangquan coalfield is one of the most important anthracite coal bases in China. Its annual gas emission accounts for about one-sixth of China's total gas emission, and most of its coal seams are outburst seams. All the coal samples used in this paper were taken from #8 coal samples, larger than 300 mm in diameter, at the newly exposed tunneling face. They were wrapped and sealed in paper and black plastic bags and then transported to the ground. According to the standards of coal experiments [21], the coal block was processed into cubic coal samples of $50 * 50 * 50\ \text{mm}^3$. Then each surface was sanded and leveled with the abrasive paper to avoid secondary damage as much as possible, until the requirements for samples were met. Next, samples were ground, until the nonparallelism of the surfaces on both ends was less than 0.05 mm. Finally, five standard #8 coal samples were processed, as shown in Figure 2.

In Figure 1, x and y denote the two directions parallel to the coal seam and z refers to the direction vertical to the coal seam.

The size of coal samples is measured by a vernier caliper, and the density is measured by the drainage method [22]. Ash, moisture, and volatile matter of coal samples could be

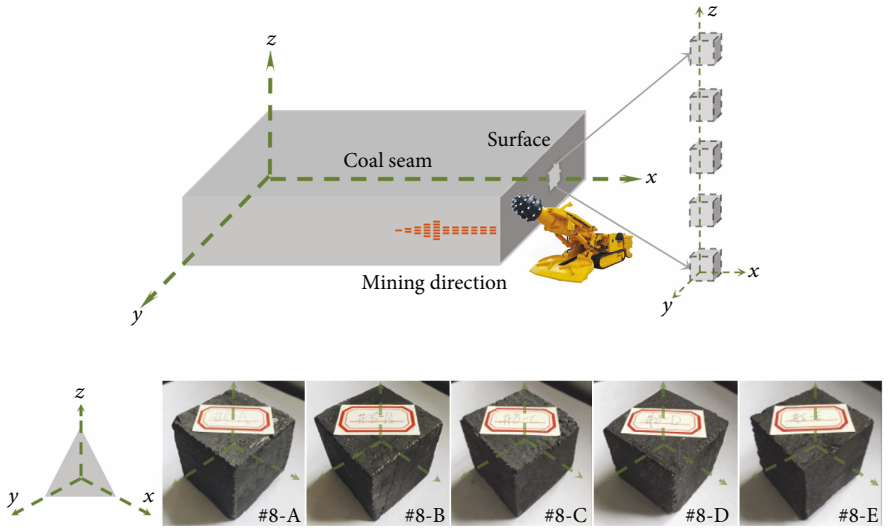

Figure 2: Schematic diagram of coal sample acquisition.

Table 1: Basic parameters of coal samples.

Sample ID	Size ($x * y * z$) (mm^3)	ρ (g/mm^3)	M_{ad}	A_{ad}	V_{dnf}	a	b
#8-A	50.02 * 50.00 * 50.04	1.62	2.00	10.32	10.29	33.73	1.42
#8-B	49.96 * 50.04 * 50.01	1.60	1.98	10.37	10.25	33.69	1.41
#8-C	49.99 * 50.02 * 50.02	1.61	1.99	10.37	10.18	33.71	1.42
#8-D	50.05 * 49.99 * 50.01	1.63	2.01	10.25	10.35	33.77	1.45
#8-E	50.02 * 50.03 * 49.97	1.59	1.98	10.41	10.20	33.67	1.40

obtained by industrial analysis of coal [23]. Adsorption constants (a and b) of #8 coal samples were obtained by isothermal adsorption experiment [24]. The basic parameters of coal samples are shown in Table 1.

2.2. Experimental Apparatus and Experimental Error Analysis. The ultrasound pulse transmission method is used in the experiment [25, 26]. The acoustic signals of coal samples are collected by DB16A multichannel ultrasonic instrument. The sampling frequency is 100 kHz. The velocities (P- and S-waves) of coal samples can be calculated as follows [27, 28]:

$$V_P = \frac{L}{t_P - t_0}, \quad V_S = \frac{L}{t_S - t_0}, \tag{1}$$

where V_P and V_S are the velocities (P- and S-waves), in m/s; L denotes the length of samples, in m; t_P, t_S are the first arrival time of signals, in s; t_0 is the docking time of transducers, in s.

Test errors are inevitable due to the experimental method and human factors [16], which may influence the test results. The error calculation is shown as equations 2 and 3:

$$\Delta V = \frac{\Delta L}{t - t_0} + L\left|\frac{\Delta t}{(t - t_0)^2}\right| + L\left|\frac{\Delta t_0}{(t - t_0)^2}\right|, \tag{2}$$

$$E = \frac{\Delta V}{V} \times 100\%, \tag{3}$$

where ΔV denotes the error of velocity, in m/s; $t - t_0$ is the travel time of signals, in s; Δt is the picking error, in s; Δt_0 is the error of docking time, in s; L and ΔL are the length and length error of coal samples, in m; E stands for the velocity error.

Δt and Δt_0 of the ultrasonic speed experiment are set at the value of 0.1 μs based on the sampling interval (0.1 μs). ΔL is the length error, being less than 0.05 mm. For example, the first arrival time of the signals of the coal samples is about 30 μs. The errors in actual measurement also include calibration errors and data reading errors. Therefore, according to equation (3), the velocity errors may change but only by $E \leq 1.2\%$.

2.3. Experimental Procedure. As shown in Figure 3, the test is carried out by using the gas-bearing coal ultrasonic test system in the State Key Laboratory of Coal Resources and Safe Mining of China University of Mining and Technology (CUMT). The system can be used to test the

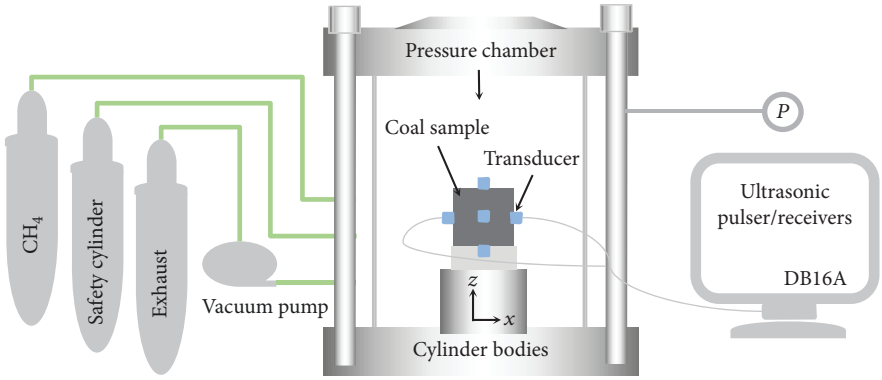

Figure 3: Ultrasound anisotropy testing system of coal samples (simplified).

ultrasonic velocity of coal under different gas pressure conditions. Then the ultrasonic elastic response and anisotropic characteristics of coal samples under different gas pressure conditions are revealed. In the test, the gas pressure is loaded in an isogradient manner. The specific test procedure is shown as follows.

(1) The experiment is conducted under normal temperature and atmospheric pressure (298 K, 1 atm)

(2) To ensure the coupling between the probe and the sample surface, the Shear Gel is applied on the probe surface after the prepared sample is put into the coal clamp and then covered with the top lid

(3) To check the air tightness of the system, it is observed whether the piezometer reading is changed or not. A vacuum pump is used to vacuum the sealed cylinder block. When the negative pressure in the chamber is stabilized at -0.1 MPa, the vacuum should be stopped. The acoustic signals in the x and y directions and in the z direction under the negative pressure condition are collected by three ultrasonic transducers

(4) When the vacuum test is finished, the cylinder body is filled slowly with the high-pressure mixture gas ($CO_2$60% + N_2 40%) instead of CH_4 gas in an isogradient manner through the pressure relief valve to a predetermined pressure value (-0.1-1.4 MPa) [29]. This operation can be justified by the fact that according to laboratory safety regulations, the use of CH_4 gas is prohibited during the experiment and that the abovementioned mixed gas has similar adsorption effect with CH_4 gas [30]. Then the air tightness of the system is checked again. After the gas reaches the adsorption equilibrium and the preset pressure value is maintained for 24 hours, the acoustic signals of the samples under different gas pressures are finally collected. Based on Langmuir isothermal adsorption equation (4) [24], the gas adsorption capacity of coal samples under different pressure equilibrium conditions can be estimated, as shown in Table 2 and Figure 4. It should be mentioned that the pure component isotherm is empirically used to describe an actual binary system, thus neglecting any competitive adsorption of CO_2 and N_2

Table 2: Gas adsorption capacity of coal samples under different gas pressure conditions.

P (MPa)	Q (ml/g)				
	#8-A	#8-B	#8-C	#8-D	#8-E
-0.1	0	0	0	0	0
0.2	7.46	7.41	7.46	7.59	7.37
0.4	12.22	12.15	12.21	12.40	12.09
0.6	15.52	15.44	15.51	15.71	15.37
0.8	17.94	17.86	17.93	18.14	17.79
1.0	19.79	19.71	19.78	19.99	19.64
1.2	21.26	21.18	21.24	21.45	21.11
1.4	22.44	22.36	22.43	22.62	22.30

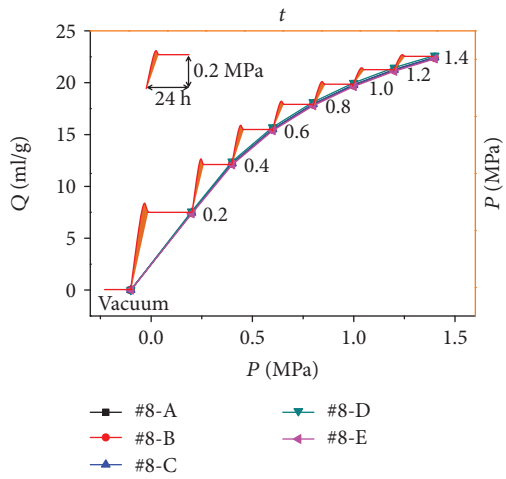

Figure 4: Deformation curves of isogradient pressurized adsorption and gas adsorption capacity of the coal samples.

$$Q = \frac{a \cdot b \cdot P}{1 + b \cdot P}, \quad (4)$$

Table 3: Test results of P- and S-wave ultrasonic velocities of the coal samples under different gas pressures.

P (MPa)	V_P (m/s)			V_S (m/s)		
	x	y	z	x	y	z
-0.1	1793	1733	1677	982	926	871
0.2	1733	1673	1650	959	911	863
0.4	1706	1653	1635	951	905	858
0.6	1691	1644	1627	947	901	851
0.8	1683	1635	1614	943	897	847
1.0	1675	1629	1607	937	893	845
1.2	1664	1621	1600	933	889	841
1.4	1652	1613	1596	927	886	841

where Q denotes the gas adsorption capacity of the coal sample, in ml/g; P is the pressure of gas, in MPa; a and b are the adsorption constants of the coal sample.

As can be seen from Figure 4, with the increase of gas pressure, the gas adsorption capacity of five coal samples is also increasing gradually, but the rising trend becomes milder in the later phase

(5) The signals collected are calculated, processed, and analyzed (refer to Section 2.2)

3. Test Results and Discussion

3.1. Ultrasonic Velocity of Gas-Bearing Coal Samples. Since the five anthracite samples are all taken from large coal samples from the same coal seam, the measured ultrasonic velocity values can denote the comprehensive response values of various material components, pore structure, and bedding plane of coal. Therefore, the average value of the ultrasonic velocity data of the five anthracite samples is analyzed and the analysis results (shown in Table 3) can reflect the general characteristics of #8 anthracite.

The ultrasonic elasticity test indicates that the ultrasonic velocity of coal samples shows similar downward trends with the increase of gas pressure. As shown in Figures 5(a) and 5(b), the V_P of anthracite coal samples is about 1600-1800 m/s while the V_S is within the interval of 800-1000 m/s. Compared with the previous research results [14–19, 31–33], the ultrasonic velocity results of the coal samples in this study are within a reasonable range.

According to the results of previous researches [14–19, 31–33], the V_P and V_S of the coal samples are the comprehensive response value of geological parameters such as material composition, pore structure, and environment of coal itself. The density, temperature, stress, and water of coal all influence the ultrasonic wave velocity of coal [17]. However, the five coal samples used in this experiment are all taken from the same position and the experiment is carried out under the same normal temperature and pressure. Therefore, it can be concluded that the density, temperature, stress, and moisture of coal samples cannot be the main factors leading to the above changes [34–36].

The adsorption of gas leads to a decrease in the strength of coal samples [37], which can be reflected in the variation of the V_P and V_S.

3.2. Variation in Ultrasonic Velocity of Coal Samples under Different Gas Pressures. From Figure 6, it can be seen that components of V_P and V_S of the coal samples are very different in the three directions, and meanwhile, their degree of decline varies from one another as the gas pressure increases.

Specifically, as shown in Figures 6(a) and 6(b), V_P and V_S of the coal samples decrease in turn in the strike direction x, the dip direction y, and the vertical direction z. However, in Figures 5(a) and 5(b), it can be seen that the correlation coefficient $R_z^2 = 0.95$ between ultrasonic velocity and gas pressure in the vertical direction z is significantly higher than that in the strike direction x and the dip direction y. Therefore, the clay and pore fracture of coal may be the main cause for this phenomenon. Meanwhile, with the increase of gas pressure, V_P and V_S of the coal samples show a noticeable downward trend, in which V_P decreases by 7.86%, 6.92%, and 4.83% in the strike direction x, the dip direction y, and the vertical direction z, respectively, while V_S decreases by 5.6%, 4.53%, and 3.44%, respectively, in the corresponding three directions. The P-wave, especially high-frequency ultrasonic P-wave, is more sensitive to gas pressure changes, which may be justified by the strong absorption and attenuation of ultrasonic elastic waves by gas-bearing coal fluid-solid two-phase medium.

Previous studies [37–40] have shown that the adsorption and desorption of coal samples are physical phenomena. When the coal samples absorb gas, they undergo expansion. On the contrary, compression deformation occurs after gas is desorbed. The deformation firstly weakens the strength of the coal samples and increases the brittleness of the coal samples, making the coal more prone to instability and damage. Then the instability and failure process of the coal samples are to be accelerated, leading to the decrease of coal sample strength and the increase of brittleness. In the meanwhile, along with the phenomena of gas adsorption and expansion deformation of the coal samples, there is a size effect on the coal samples—to be specific, the volume of the coal sample increases (adsorption expansion). Therefore, in the calculation of ultrasonic velocity of the coal samples, the proportion of the volume increase caused by the adsorption and expansion is analyzed below.

According to the existing research, under the constant gradient pressure conditions, the adsorption expansion deformation of coal samples increases as time goes by but the cumulative deformation eventually tends to remain at a stable value. The isocratic pressure in the reference [40] is set to a value of 1.5 MPa. The microstrain of cumulative adsorption expansion is achieved under the condition of adsorption equilibrium. According to the reference [41], the maximum deformation of the coal sample used in the experiment can be calculated by the calculation formula of the coal adsorption deformation equation.

$$\varepsilon = \frac{ABP}{1 + BP}, \tag{5}$$

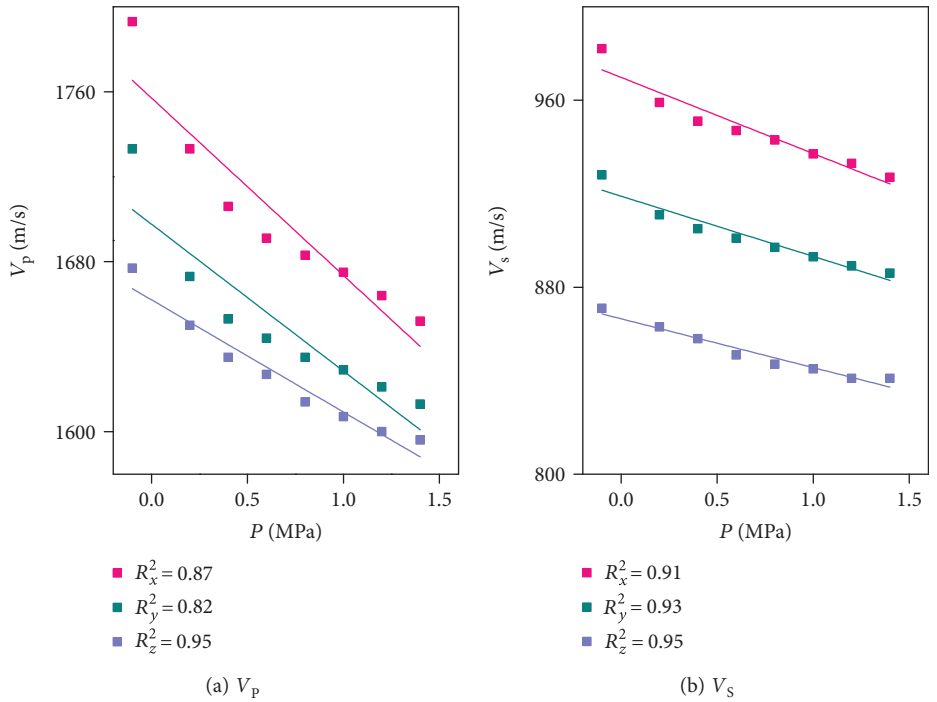

Figure 5: Characteristic charts of ultrasonic velocity of coal samples at different gas pressures.

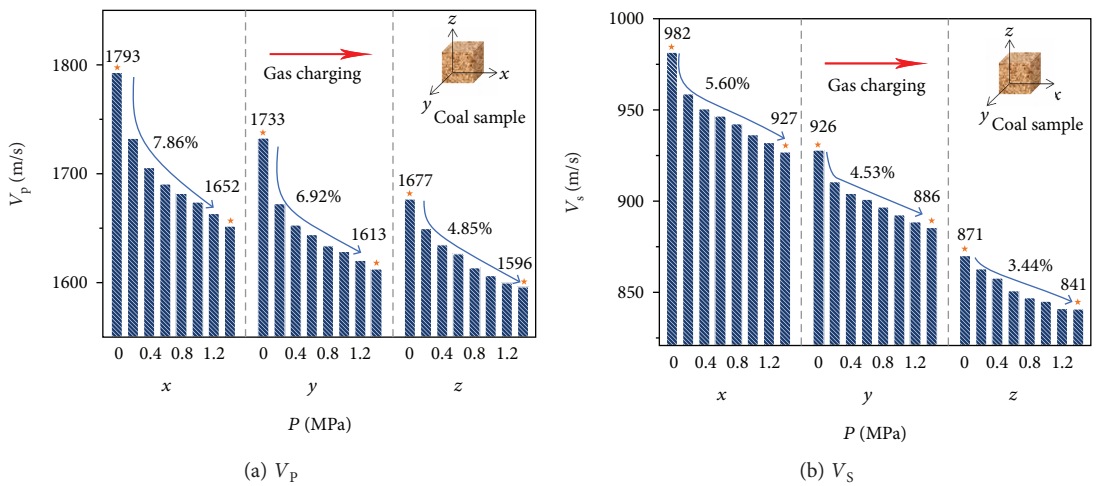

Figure 6: Measured V_P and V_S.

where ε denotes the adsorption deformation quantity of the coal sample, in ‰; P is the gas pressure, in MPa; A is the limit adsorption deformation constant of the coal sample when gas pressure tends to be infinite, in ‰; B is the adsorption deformation constant of the coal sample, in MPa^{-1}.

Table 4 shows that the maximum adsorption deformation quantity of the gas-bearing coal sample in the calculation of coal ultrasonic velocities is only 2.99‰, so the effect of gas adsorption deformation on anthracite samples is small.

The gas-bearing coal sample is a typical fluid-solid two-phase and two-porosity medium, and the sample is composed of solid skeleton, pore, fracture, and gas filled in the pore and fracture [42]. There exist three kinds of compressional wave (P-wave and two slow compressional waves P_2 and P_3) and S-wave. The velocity of the P-wave is the fastest,

Table 4: Adsorption deformation constant and quantity of coal samples.

Sample ID	A (‰)	B (MPa^{-1})	ε (‰)
#8-A	3.704	2.250	2.81
#8-B	3.563	2.198	2.69
#8-C	3.624	2.283	2.76
#8-D	3.926	2.277	2.99
#8-E	3.677	2.221	2.78

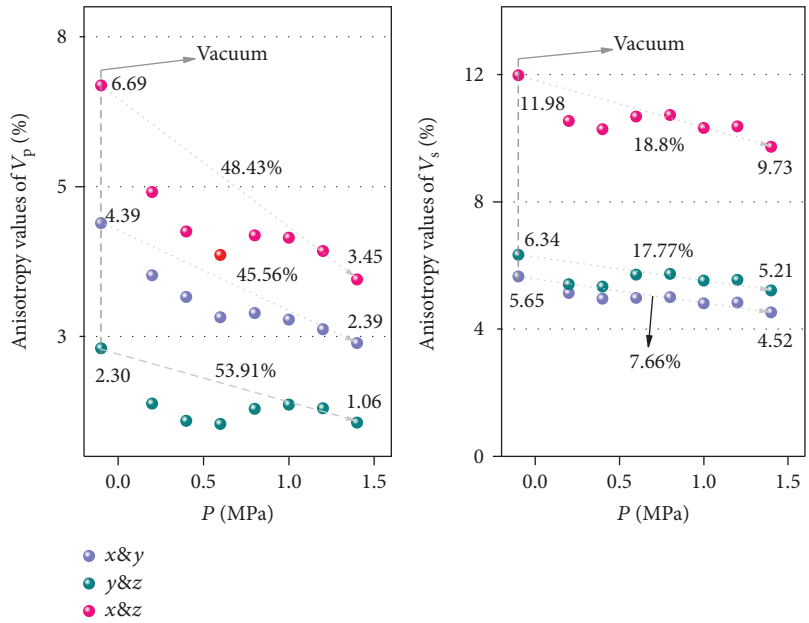

Figure 7: Anisotropy of V_P and V_S of coal samples.

the S-wave ranks second, and P_2 and P_3 are the slowest [43]. The P-wave and S-wave propagate in the skeleton. Slow compressional wave P_2 is produced by the interaction of the solid skeleton and gas in the pore, and slow compressional wave P_3 is produced by the interaction of the solid skeleton and gas in the fracture.

In this paper, only the P-wave and S-wave are studied. Accordingly, the influence factor of P-wave and S-wave velocity variations only includes the solid skeleton. On the one hand, the skeleton deformation is caused by gas adsorption. In the previous study, the effect of gas adsorption deformation on anthracite samples is small, so adsorption deformation has little effect on the wave velocity of anthracite samples. On the other hand, with the increase of gas pressure, adsorbed quantity of gas increases and adsorbed quantity of gas on the skeleton surface increases, which in turn leads to the decrease of solid skeleton strength. Ultimately, the velocities of the P- and S-wave decrease with the increase of gas pressure.

3.3. Anisotropy Characteristics of Velocity. It is known that with the increase of gas pressure, V_P and V_S of the coal samples decrease. Meanwhile, the velocity (P- and S-waves) distribution of the coal samples exhibits different characteristics in the three directions. So, the influence of gas pressure on the ultrasonic velocity anisotropy of anthracite is analyzed in this section and the velocity anisotropy values of selected coal samples can be calculated with the following formulas [17].

$$AV_P = \frac{2(V_P(\max) - V_P(\min))}{(V_P(\max) + V_P(\min))} \times 100\%,$$
$$AV_S = \frac{2(V_S(\max) - V_S(\min))}{(V_S(\max) + V_S(\min))} \times 100\%, \quad (6)$$

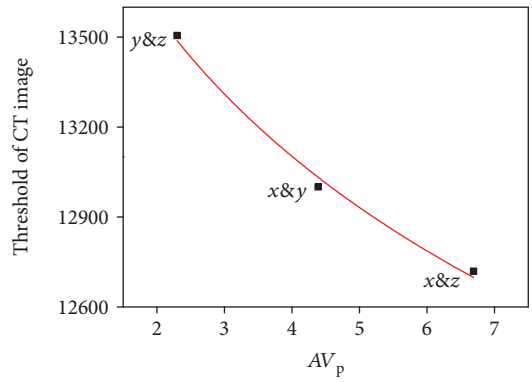

Figure 8: The relation between CT image threshold and anisotropic value from different views.

where AV_P and AV_S denote the anisotropy values of velocities (P-wave and S-wave, respectively). The results obtained are shown in Figure 7.

As can be seen from Figure 7, when the coal samples are under vacuum (negative pressure), the anisotropy between x and z is greater than those between x and y and y and z. Through X-ray tomography of coal samples, the CT digital images of coal samples can be obtained in order to interpret the differences in the above directions [44, 45]. The test was carried out on Xradia 510 Versa high-resolution three-dimensional X-ray microimaging system (3D-XRM). The correlation between CT image thresholds from three views and three anisotropic values of P-wave velocity can be established; as shown in Figure 8, there is a negative correlation between them. It can be seen that there is a logarithmic negative correlation between them. The threshold of CT images from the x and z views shows that the average density of clays and pore fractures is the smallest, which leads to the maximum anisotropy between x and z. The main cause of

the abovementioned directional differences may be the inconsistency between the clays and the pore fractures of the coal [14–19].

With the increase of gas pressure, the anisotropy of wave velocity of coal samples keeps the same difference as that of vacuum but decreases gradually on the whole and the decrease of P-wave velocity anisotropy is much larger than that of S-wave velocity anisotropy. Specifically, the decreases of P-wave velocity anisotropy in the strike direction x, the dip direction y, and the vertical direction z are 45.56%, 48.43%, and 53.91%, respectively, while the decreases of S-wave velocity anisotropy are only 7.66% (x and y), 18.8% (x and z), and 17.77% (y and z), respectively. It can be concluded that the anisotropy of P-wave velocity decreases much more than that of the S-wave, which indicates that the P-wave is more sensitive to gas pressure changes.

Therefore, the most possible cause is that the coal samples undergo adsorption due to the existence of fluid gas [37, 46]. As a result, the strength of the coal samples is weakened and the strong ultrasonic anisotropy of the coal samples is also gradually weakened under the action of the high-pressure gas adsorption expansion.

4. Conclusions

Many achievements have been made in the ultrasonic elasticity test of single-phase solid coal seam. However, in the actual gas geological condition, coal seam is not a single solid medium but a two-phase and two-porosity. So, the ultrasonic velocity and anisotropy of gas-bearing coal two-phase and two-porosity are studied in this paper. Relevant results can be mainly applied in seismic exploration of a high-gas mine, which can provide theoretical guidance for the prediction and prevention of coal and gas disasters by identifying abnormal areas of gas enrichment in seismic exploration. Finally, the following conclusions can be drawn.

(1) In the strike, dip, and vertical directions, there is a negative linear relationship between the ultrasonic velocity and gas pressure. It is manifested by the fact that the ultrasonic velocity (P-wave and S-wave) decreases with the increase of gas pressure. As for the cause of this phenomenon, it can be concluded that the increase of gas pressure leads to the increase of gas adsorption quantity on the skeleton surface, causing the decrease of skeleton strength, and resulting in the decrease of P-wave and S-wave velocities propagating in the solid skeleton of gas-bearing coal samples. Moreover, the correlation coefficient between the ultrasonic velocity and the gas concentration in the vertical direction is significantly higher than that in the strike direction and the dip direction

(2) The degree of S-wave anisotropy is greater than that of the P-wave. In addition, $AV_P(x\&z)$ is greater than $AV_P(x\&y)$ and $AV_P(y\&z)$; $AV_S(x\&z)$ is greater than $AV_S(x\&y)$ and $AV_S(y\&z)$. With the increase of gas pressure, the anisotropy of velocities (P- and S-waves) of coal samples decreases stepwise as a whole

(3) The decrease in P-wave velocity and its anisotropy is greater than that in the S-wave, which indicates that P-wave velocity is more sensitive to gas pressure changes

In the actual seismic exploration, under the constraints of drilling and logging, the above laws of the ultrasonic anisotropy of the coal samples affected by gas may provide some theoretical guidance for the prevention of gas disasters.

Data Availability

The data used to support the findings of this study are available from the corresponding author upon request. The data of this manuscript is based on previous studies and obtained through experiments in the laboratory. Therefore, the data in this paper are all first-hand data and the data are guaranteed to be true and reliable.

Conflicts of Interest

The authors declare no conflict of interest.

Acknowledgments

This paper is supported by the National Natural Science Foundation of China (nos. 41604082 and 51734009), the Independent Innovation Project for Double First-level Construction (China University of Mining and Technology) (no. 2018ZZCX04) and the National Key R&D Program of China (no. 2018YFC0807802).

Supplementary Materials

Table 4: (Section 3.3 of the corresponding manuscript, Figure 7). *(Supplementary Materials)*

References

[1] J. Sobczyk, "A comparison of the influence of adsorbed gases on gas stresses leading to coal and gas outburst," *Fuel*, vol. 115, no. 2, pp. 288–294, 2014.

[2] X. Xu, R. Zhang, F. Dai, B. Yu, M. Gao, and Y. Zhang, "Effect of coal and rock characteristics on ultrasonic velocity," *Journal of China Coal Society*, vol. 40, no. 4, pp. 793–800, 2015.

[3] X. Liu, X. Wang, E. Wang, Z. Liu, and X. Xu, "Study on ultrasonic response to mechanical structure of coal under loading and unloading condition," *Shock and Vibration*, vol. 2017, Article ID 7643451, 12 pages, 2017.

[4] Y. Chen, T. F. Huang, and E. R. Liu, *Rock Physics*, Press of University of Science and Technology of China, Hefei, China, 2009.

[5] State Administration of Work Safety, *National Coal Mine Safety Administration, regulations on prevention and control of coal and gas outburst*, China Coal Industry Publishing House, Beijing, China, 2009.

[6] N. I. Aziz and W. Ming-Li, "The effect of sorbed gas on the strength of coal – an experimental study," *Geotechnical & Geological Engineering*, vol. 17, no. 3/4, pp. 387–402, 1999.

[7] S. Wang, D. Elsworth, and J. Liu, "Mechanical behavior of methane infiltrated coal: the roles of gas desorption, stress level and loading rate," *Rock Mechanics and Rock Engineering*, vol. 46, no. 5, pp. 945–958, 2013.

[8] L. Zhang, N. Aziz, T. Ren, J. Nemcik, and S. Tu, "Influence of coal particle size on coal adsorption and desorption characteristics," *Archives of Mining Sciences*, vol. 59, no. 3, pp. 807–820, 2014.

[9] S. D. Liu, Q. F. Zhao, P. S. Zhang, and L. Q. Guo, "Test and research on relationship between seam gas features and vibration wave parameters," *Coal Science and Technology*, vol. 33, no. 11, pp. 33–36, 2005.

[10] X.-P. Chen, Q. Huo, J. Lin et al., "The inverse correlations between methane content and elastic parameters of coal-bed methane reservoirs," *Geophysics*, vol. 78, no. 4, pp. D237–D248, 2013.

[11] L. Mei, G. Jingwei, Y. Guangming, and L. Jiandong, "Application of seismic anisotropy caused by fissures in coal seams to the detection of coal-bed methane reservoirs," *Acta Geologica Sinica - English Edition*, vol. 74, no. 2, pp. 425–428, 2000.

[12] A. Morcote, G. Mavko, and M. Prasad, "Dynamic elastic properties of coal," *Geophysics*, vol. 75, no. 6, pp. E227–E234, 2010.

[13] S. H. Dong, H. B. Wu, D. H. Li, and Y. P. Huang, "Experimental study of ultrasonic velocity and anisotropy in coal sample," *Journal of Seismic Exploration*, vol. 25, no. 2, pp. 131–146, 2016.

[14] Z. Wang, "Seismic anisotropy in sedimentary rocks, part 2: Laboratory data," *Geophysics*, vol. 67, no. 5, pp. 1423–1440, 2002.

[15] H. Wu, S. Dong, D. Li, Y. Huang, and X. Qi, "Experimental study on dynamic elastic parameters of coal samples," *International Journal of Mining Science and Technology*, vol. 25, no. 3, pp. 447–452, 2015.

[16] H. Chen, B. Jiang, T. Chen, S. Xu, and G. Zhu, "Experimental study on ultrasonic velocity and anisotropy of tectonically deformed coal," *International Journal of Coal Geology*, vol. 179, pp. 242–252, 2017.

[17] Y. Wang, X. K. Xu, and Y. G. Zhang, "Characteristics of P-wave and S-wave velocities and their relationships with density of six metamorphic kinds of coals," *Chinese Journal of Geophysics*, vol. 55, no. 11, pp. 3754–3761, 2012.

[18] S. H. Dong and W. P. Tao, "Test on elastic anisotropic coefficients of gas coal," *Chinese Journal of Geophysics*, vol. 51, no. 3, pp. 671–677, 2008.

[19] Q. Zhao and S. L. Hao, "Anisotropy test instance of ultrasonic velocity and attenuation of coal sample," *Progress in Geophysics*, vol. 21, no. 2, pp. 531–534, 2006.

[20] Y. Wang, X. K. Xu, and D. Y. Yang, "Ultrasonic elastic characteristics of five kinds of metamorphic deformed coals under room temperature and pressure conditions," *Science China Earth Sciences*, vol. 57, no. 9, pp. 2208–2216, 2014.

[21] R. Ulusay, *The ISRM Suggested Methods for Rock Characterization, Testing and Monitoring: 2007–2014*, Springer International Publishing, 2015.

[22] J. L. Wang, Y. P Long, and C. S. Zhu, *The National Standards Compilation Group of Peoples Republic of China, GB/T 6949-2010 Determination of Apparent Relative Density of Coal*, Standards Press of China, Beijing, China, 2011.

[23] L. T. Han, Y. J. Lin, and K. Q. Chen, *The National Standards Compilation Group of Peoples Republic of China, GB/T 212-2008 Industrial Analysis Method of Coal*, Standards Press of China, Beijing, China, 2008.

[24] D. M. Ma, S. A. Zhang, and Y. B. Lin, "Isothermal adsorption and desorption experiment of coal and experimental results accuracy fitting," *Journal of the China Coal Society*, vol. 36, no. 3, pp. 477–480, 2011.

[25] R. Simm and M. Bacon, *Seismic Amplitude: An interpreter's Handbook*, Cambridge University Press, 2014.

[26] G. Mavko, T. Mukerji, and J. Dvorkin, *The Rock Physics Handbook*, Cambridge University Press, 2009.

[27] R. Tonn, "The determination of the seismic quality factor Q from VSP data: a comparison of different computational methods," *Geophysical Prospecting*, vol. 39, no. 1, pp. 1–27, 1991.

[28] Y. Wang, J. Lu, Y. Shi, and C. Yang, "PS-wave Q estimation based on the P-wave Q values," *Journal of Geophysics and Engineering*, vol. 6, no. 4, pp. 386–389, 2009.

[29] Q. H. Zhang, H. P. Wang, S. C. Li et al., "Exploration of similar gas like methane in physical simulation test of coal and gas outburst," *Rock and Soil Mechanics*, vol. 38, no. 2, pp. 479–486, 2017.

[30] S. Ottiger, R. Pini, G. Storti, and M. Mazzotti, "Measuring and modeling the competitive adsorption of CO_2, CH_4, and N_2 on a dry coal," *Langmuir*, vol. 24, no. 17, pp. 9531–9540, 2008.

[31] Z. Wang, "Fundamentals of seismic rock physics," *Geophysics*, vol. 66, no. 2, pp. 398–412, 2001.

[32] S. Peng, H. Chen, R. Yang, Y. Gao, and X. Chen, "Factors facilitating or limiting the use of AVO for coal-bed methane," *Geophysics*, vol. 71, no. 4, pp. C49–C56, 2006.

[33] X. C. Li, B. S. Nie, X. Q. He, X. Zhang, and T. Yang, "Influence of gas adsorption on coal body," *Journal of China Coal Society*, vol. 36, no. 12, pp. 2035–2038, 2011.

[34] H. Wang, J. Pan, S. Wang, and H. Zhu, "Relationship between macro-fracture density, P-wave velocity, and permeability of coal," *Journal of Applied Geophysics*, vol. 117, pp. 111–117, 2015.

[35] Y. G. Wang, M. G. Li, B. B. Chen, and S. H. Dai, "Experimental study on ultrasonic wave characteristics of coal samples under dry and water saturated conditions," *Journal of China Coal Society*, vol. 40, no. 10, pp. 2445–2450, 2015.

[36] Y. G. Wang, T. T. Yang, and Q. Y. Wang, "Study on ultrasonic propagation characteristics in coal samples," *China Safety Science Journal*, vol. 27, no. 12, pp. 68–73, 2017.

[37] X. Nie, J. Chen, Y. Cao, D. Gong, and H. Deng, "Analysis of coal swelling deformation caused by carbon dioxide adsorption based on X-ray computed tomography," *Geofluids*, vol. 2018, Article ID 6939827, 11 pages, 2018.

[38] Y. Zhang, M. Lebedev, M. Sarmadivaleh, A. Barifcani, and S. Iglauer, "Swelling-induced changes in coal microstructure due to supercritical CO_2 injection," *Geophysical Research Letters*, vol. 43, no. 17, pp. 9077–9083, 2016.

[39] S. Day, R. Fry, and R. Sakurovs, "Swelling of Australian coals in supercritical CO_2," *International Journal of Coal Geology*, vol. 74, no. 1, pp. 41–52, 2008.

[40] Z. G. Zhang, S. G. Cao, and P. Guo, "Comparison of the deformation characteristics of coal in gas adsorption-desorption process for raw and briquette coals," *Journal of China University of Mining & Technology*, vol. 43, no. 3, pp. 388–394, 2014.

[41] Y. A. Wang and Y. M. Tao, "Adsorption deformation and adsorption deformation force of coal," *Coal Mine Safety*, vol. 6, pp. 19–26, 1993.

[42] Y. Wu, J. Liu, D. Elsworth, Z. Chen, L. Connell, and Z. Pan, "Dual poroelastic response of a coal seam to CO_2 injection," *International Journal of Greenhouse Gas Control*, vol. 4, no. 4, pp. 668–678, 2010.

[43] J. G. Berryman and H. F. Wang, "Elastic wave propagation and attenuation in a double-porosity dual-permeability medium," *International Journal of Rock Mechanics and Mining Sciences*, vol. 37, no. 1-2, pp. 63–78, 2000.

[44] L. Pimienta, L. Esteban, J. Sarout et al., "Supercritical CO_2 injection and residence time in fluid-saturated rocks: evidence for calcite dissolution and effects on rock integrity," *International Journal of Greenhouse Gas Control*, vol. 67, pp. 31–48, 2017.

[45] G. Wang, J. N. Shen, X. Y. Chu, X. Y. Cao, C. H. Jiang, and X. H. Zhou, "Characterization and analysis of pores and fissures of high-rank coal based on CT three dimensional reconstruction," *Journal of China Coal Society*, vol. 42, no. 8, pp. 2074–2080, 2017.

[46] Y. B. Liu, S. G. Cao, Y. Li et al., "Experimental study of swelling deformation effect of coal induced by gas adsorption," *Chinese Journal of Rock Mechanics and Engineering*, vol. 29, no. 12, pp. 2484–2491, 2010.